



# Design and analysis of RF MEMS shunt switch for V-band applications

K. Srinivasa Rao<sup>1</sup> · T. Madhuri<sup>1</sup> · Leela Krishna<sup>1</sup> · T. Manish Sairam<sup>1</sup> · Shaik Shoukath Vali<sup>1</sup> · Ch. Gopi Chand<sup>3</sup> · K. Girija Sravani<sup>1,2</sup>

Received: 25 November 2021 / Accepted: 8 April 2022 / Published online: 3 May 2022  
© The Author(s), under exclusive licence to Springer-Verlag GmbH Germany, part of Springer Nature 2022

## Abstract

In this paper, we have designed and simulations of RF MEMS shunt switch. The electro-mechanical and electromagnetic analysis of the switch have been done using COMSOL Multi-physics and HFSS tools. Here, we have designed and simulated the switch with different beam materials of gold, silver, aluminium, and the dielectric material is taken as Si<sub>3</sub>N<sub>4</sub>. The pull-in-voltage acquired for gold material is 3.3 V an air gap of 2 μm which is efficient when contrast with other materials like silver and aluminium. The up and downstate capacitance of the switch is 48fF and 1.19 pF. By using HFSS (High-Frequency Structure Simulator) software we have performed the RF performance analysis such as isolation, insertion, and return losses were measured. The return and insertion losses are − 16.71, − 2.69 dB, and isolation of − 29.39 dB at 40–75 GHz, so the switch is used for V-band applications.

## 1 Introduction

A micro-electro-mechanical system (MEMS) is miniaturized mechanical moving parts and elements of electronic segments on a single module chip. In recent years RF MEMS switches widely used in different band applications. Nowadays capacitive shunt switches have create a significant part in the growth of advanced communication applications. Capacitive MEMS switches are preferred for filter design, reconfigurable microwave antennas, and space applications. (Dussopt and Rebeiz 2003; Bakri-Kassem and Mansour 2014; Sharma et al. 2020). V-band has been used for short line of sight terrestrial application because the frequency is very high to penetrate. Here users of the V-band is directly connected to the communication satellite with the help of the v-band switch. We can implement the RF MEMS switch in the satellite then we get V-band user links by (by directional) (Demirel et al. 2015). We can

implement the RF MEMS switch in the satellite then we get V-band user links by (by-directional). Nowadays capacitive shunt switches have a prominent part in developing in communication applications, these switches are divided as shunt and series configuration, as a capacitive and resistive switch based upon the contact. For low-frequency applications the series type switches are used, but it have poor isolation, for higher frequency applications the shunt switches are utilized (Vu et al. 2012; Ansari and Khosroabadi 2019; Naji et al. 2019; Rao et al. 2019). There is a lot of scope for designing these shunt switches in wireless and space applications, particularly high-frequency bands.

The V-band challenge is to model a capacitive MEMS switch for Ka-band applications because the working frequency is the target for the 10–40 GHz band. The switch shows an actuation voltage of about 9.2 V for the gold membrane. The RF characteristics are good at desired frequency range, respectively, for the dielectric layer of SiO<sub>2</sub> (Vikas et al. 2018). MEMS switch with DC contact for resonator tuning from w-band to V-band, the switch demonstrates adequate RF performance the isolation and insertion loss at 60 GHz. Characteristics brought for a device from the W-band to V-band (Chu et al. 2017). Design and optimization of a MEMS 3-port single pole double throw switch that utilized two capacitive switches. The isolation is 62 dB at 79 GHz and the insertion of − 0.12 dB at 110 GHz (Sravani et al. 2020). The return loss is about − 7 dB at excitation port more than − 10 dB

✉ T. Manish Sairam  
manishsairama@gmail.com

<sup>1</sup> Department of ECE, MEMS Research Center, Koneru Lakshmaiah Education Foundation (Deemed to be University), Green Fields, Vaddeswaram, Guntur 522502, India

<sup>2</sup> Department of ECE, NIT Silchar, Assam, India

<sup>3</sup> Department of ECE, Mizoram University (Central University), Aizwal, Mizoram, India

in or conducting port. In the above literature survey, we have observed some major limitations of the switch for the V-band (Lakshmi Narayana et al. 2017a). They have high pull-in voltage, low capacitive analysis, poor RF losses, to overcome this problem, we design an RF shunt type switch with non-uniform meandering techniques for V-band (40–75 GHz) application.

The proposed device is optimized to have a low pull-in voltage. Here we use the beam material that has gold to increase the switching speed. The use of the meanders are to decrease the pull-in voltage and to get more displacement, the voltage is applied to the electrodes (Lv and Chen 2021; Lv et al. 2021, 2022), and the simulations are done in COMSOL Multi-physics.

This paper as follows, in Sect. 2 the operation of the RF shunt switch, its dimensions, and calculated the theoretical parameters of spring constant ( $K$ ), pull-in voltage ( $V_p$ ), capacitance analysis, switching time ( $t_s$ ), and S-parameters. Section 3 expressed as results and discussions, finally in Sect. 4 concludes the paper.

## 2 Structure of proposed device

### 2.1 Operation

The proposed switch is taken as a shunt type switch., which is operated as ON and OFF state, Initially, the switch is in ON state, whenever we apply some voltage the switch will be is in OFF state, the front view in ON state as shown in Fig. 1.

When we apply the voltage on the beam, the electrostatic force is generated, directly the beam touches the dielectric then the switch is in the OFF state (Lakshmi

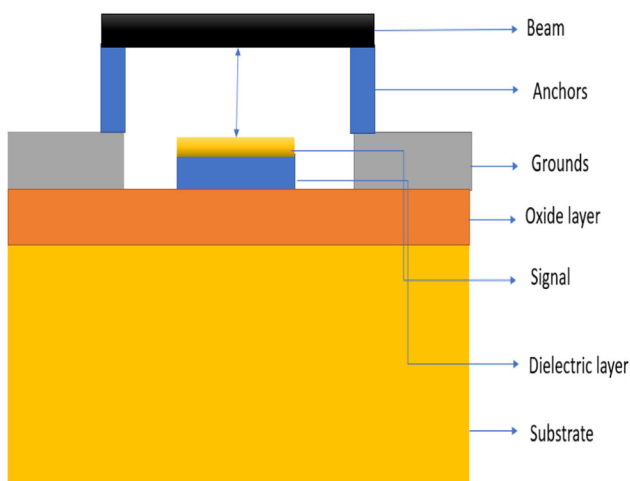


Fig. 1 ON state of the RF MEMS shunt switch

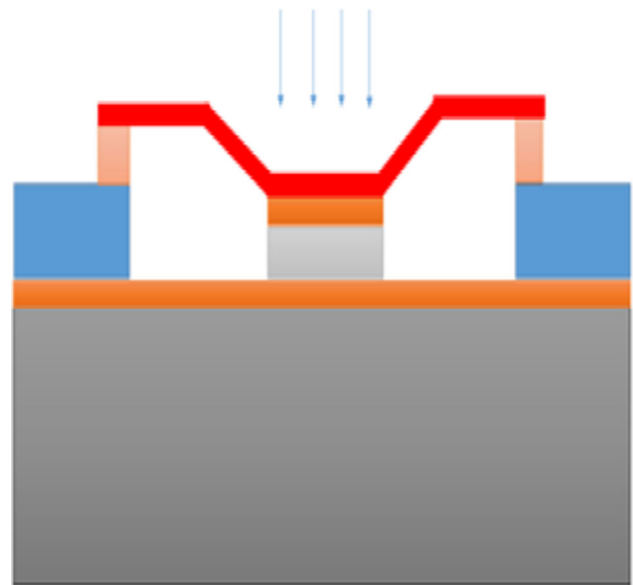


Fig. 2 Schematic of OFF state of the shunt switch

Narayana et al. 2017b; Rao et al. 2018; Sravani et al. 2019a), as shown in Fig. 2 here, there is no flow of signal input to output.

### 2.2 Proposed device

The switch is having a substrate, CPW (coplanar waveguide), an oxide layer, signal line, beam, and two anchors. Here, we have taken the shunt switch with non-uniform meanders, the schematic of a proposed switch is as shown in Fig. 3.

The proposed device is considered with silicon substrate with 720  $\mu\text{m}$  length and 400  $\mu\text{m}$  width and thickness of 10  $\mu\text{m}$ , and the dielectric is taken as 1.5  $\mu\text{m}$  thickness placed above the substrate and coplanar waveguide (CPW), which is used to communicate the signal from input to output terminals and ground. The signal dielectric is placed

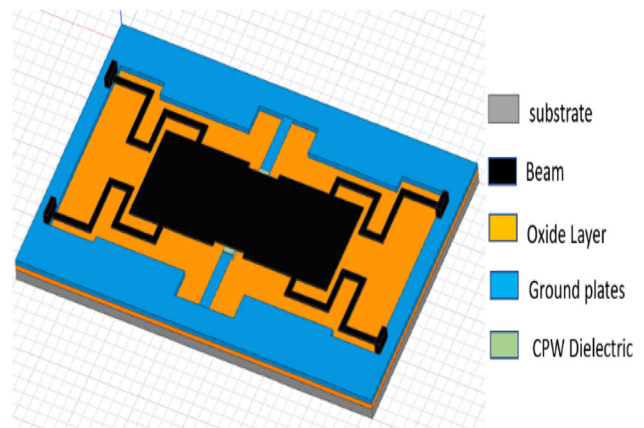


Fig. 3 3D view of proposed RF shunt switch

above the signal line, which is consists of Si<sub>3</sub>N<sub>4</sub> material, the beam is formed beyond the CPW with a gap of 3 μm, which is considered as gold material because the young’s module is less and has high conductivity compared to the other materials. The non-uniform meanders (M) are taken by reducing the spring constant and pull-in voltage, the overall dimensions of the device is given in the Table 1.

### 2.3 Theoretical parameters

#### 2.3.1 Spring constant

The mechanical moment of the switch is developed by the meanders, due to non-linear mechanical behavior. Here, we have taken the non-uniform meanders and it is calculated by using the formula is (Bansal et al. 2014) it is denoted by the letter “K”.

$$k = \frac{EWt^3}{l^3} \tag{1}$$

where ‘E’ is the young’s modulus, ‘W’ is width, ‘t’ and ‘l’—thickness and length of the beam.

#### 2.3.2 Pull in voltage

The voltage needed to operate the switch is known as pull-in voltage denoted as ‘V’, it mainly relies on the spring constant ‘K’. If the spring constant is increased as well as the pull-in voltage is also increased. It is estimated by using the formula is (Singh et al. 2013),

$$V_p = \sqrt{\frac{8Kg_0^3}{27\epsilon_0A}} \tag{2}$$

where, K—total spring constant, g<sub>0</sub>—gap, ε<sub>0</sub>—permittivity and A—actuated area.

#### 2.3.3 Capacitance analysis

Capacitance is developed between the beam and signal dielectric, through the ON and OFF state of the switch. The capacitance in upstate is calculated by the formula as (Rao et al. 2021),

$$C_u = \frac{\epsilon_0A}{g_0 + \frac{t_d}{\epsilon_r}} \tag{3}$$

In the actuated state the switch conducts as an LC resonant circuit. In OFF state the down capacitance is formed, it is calculated as,

$$C_d = \frac{\epsilon_0\epsilon_rA}{t_d} \tag{4}$$

where, A—area, g<sub>0</sub>—gap, ε<sub>0</sub>—relative permittivity, ε<sub>r</sub>—permittivity of dielectric, t<sub>d</sub>—thickness of beam.

#### 2.3.4 Switching time (t<sub>s</sub>)

The speed of the beam is deformed in active state, it is calculated by using formula as (Iannacci 2017),

$$T_s = 3.67V_p/V_s w_0 \tag{5}$$

where, V<sub>s</sub> is supply voltage, f<sub>0</sub> is resonant frequency, and V<sub>p</sub> is pull-in voltage. The angular frequency is calculated as,

$$w_0 = 2 \prod f_0 \tag{6}$$

Switching time is depending on the actuation voltage, and supply voltage the calculated switching time is 3.2 μs.

**Table 1** Dimensions of the proposed switch

Parameters	Materials	Length (μm)	Width (μm)	Height (μm)
Substrate	Silicon	720	400	10
Oxide	Silicon oxide	720	400	2
Ground	Gold	300	400	3
Signal	Gold	140	100	3
Signal dielectric	Silicon nitride	140	100	1.5
Beam	Gold	400	140	1.5
M-1	Gold	20	10	1.5
M-2	Gold	40	10	1.5
M-3	Gold	60	10	1.5
M-4	Gold	80	10	1.5

**Table 2** Spring constant and pull-in voltages for gold

Beam thickness ( $\mu\text{m}$ )	Spring constant (N/m)	Pull-in-voltage (V)
1	0.34	0.67
1.5	0.56	3.3
2	1.01	6.78
2.5	2.7	9.68
3	9.2	18.69

**Table 3** Theoretical values for aluminum

Beam thickness ( $\mu\text{m}$ )	Spring constant (N/m)	Pull-in-voltage (V)
1	0.38	4.29
1.5	0.66	5.63
2	1.3	7.88
2.5	3.08	12.15
3	10.42	22.32

**Table 4** Theoretical values for silver

Beam thickness ( $\mu\text{m}$ )	Spring constant (N/m)	Pull-in-voltage (V)
1	0.324	3.9
1.5	0.56	5.17
2	1.096	7.23
2.5	2.604	11.15
3	8.76	20.46

**Table 5** Theoretical values for copper

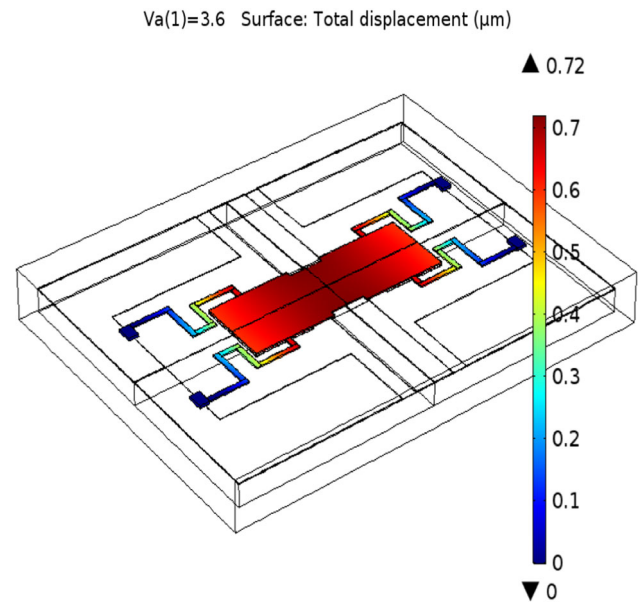
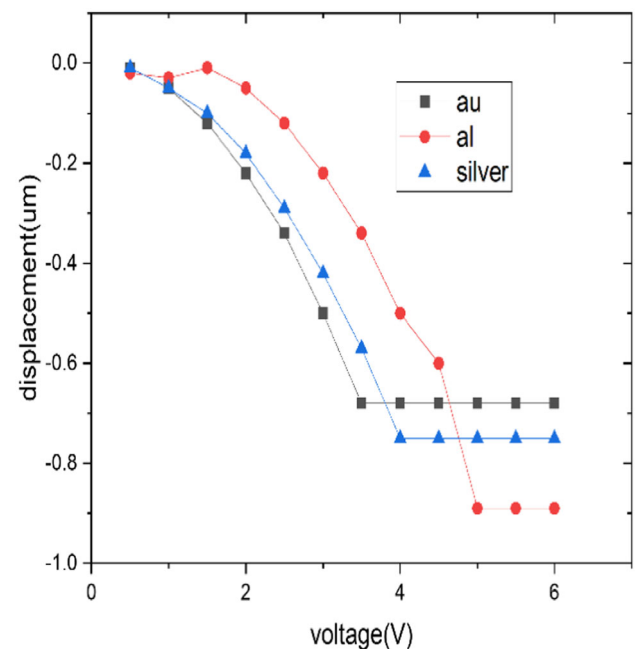
Beam thickness ( $\mu\text{m}$ )	Spring constant (N/m)	Pull-in-voltage (V)
1	0.22	4.28
1.5	0.38	5.98
2	0.75	7.87
2.5	1.78	9.23
3	6.03	16.98

## 3 Results and discussion

### 3.1 Electro-mechanical analysis

#### 3.1.1 Pull-in voltage

The theoretical calculation of spring constant and pull-in voltages are done. Here, we have calculated the different

**Fig. 4** Pull-in voltage simulation of proposed switch**Fig. 5** Voltage versus displacement of the switch with different materials

beam thickness with various materials gold, aluminum, silver, and copper, the theoretical values are shown in Table 2, 3, 4, and 5

The displacement of the switch is shown in Fig. 4, here, we have observed that at pull-in voltage of 3.3 V the displacement of a switch is 0.72  $\mu\text{m}$  with an air gap of 3  $\mu\text{m}$  and the graphical representation of voltages versus displacement with various beam materials are shown in Fig. 5.

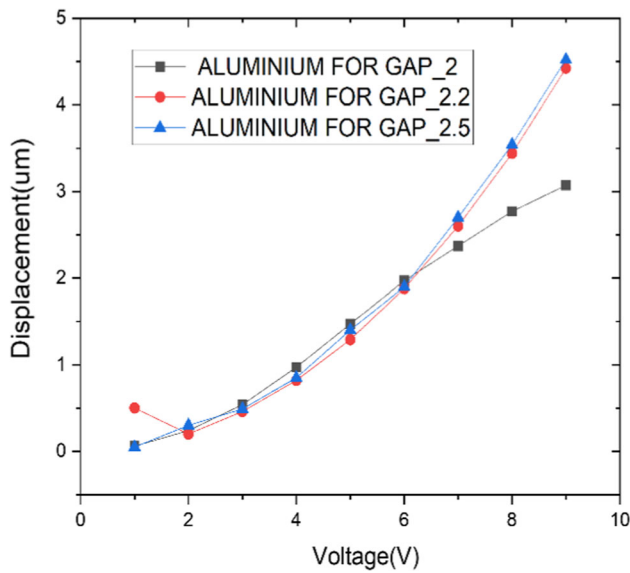


Fig. 6 Voltage versus displacement of the switch for aluminum with different air gaps

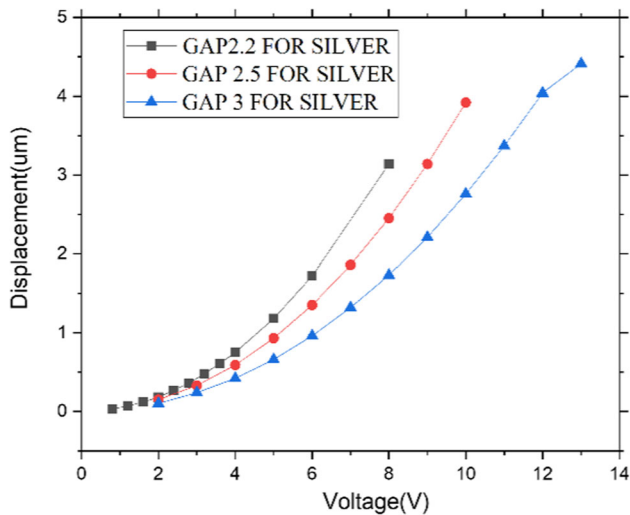


Fig. 7 Voltage versus displacement of the switch for silver with different air gaps

The theoretical and simulation results have correlated with each other. Here, we have observed that at our actuation voltage of 3.3 V the displacement has not changed it is constant as shown in Fig. 5.

The pull-in voltage analysis is done with different beam materials such as silver and aluminium, and air gaps as 2, 2.2, 2.5 μm, Figs. 6 and 7 are represented by changing the gap the displacement is increased and the pull-in voltage also increased.

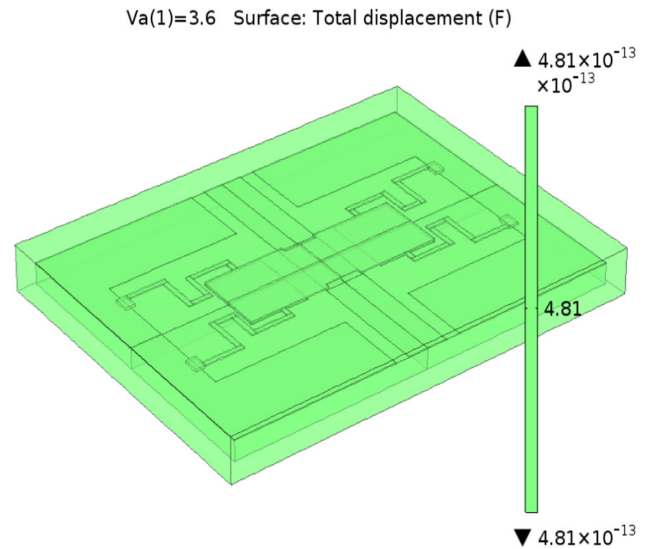


Fig. 8 Simulation of up state capacitance of the switch

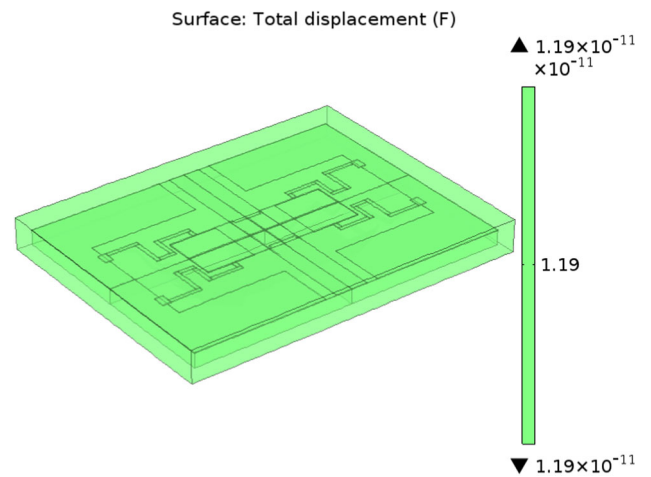


Fig. 9 Down state capacitance of the switch

### 3.1.2 Capacitance analysis

The capacitance is the main factor of the operating of the switch, the up-state capacitance is when the switch is in ON, and the downstate capacitance is when the switch is in the OFF state. The simulation result of the up-state capacitance is shown in Fig. 5, the up-state capacitance is 48 fF (Bansal et al. 2014).

The simulation result of down state capacitance is shown in Fig. 8. The down state capacitance is 1.19 pF (Fig. 9).

### 3.1.3 Stress analysis

The deformation of stress starts developing in the beam, which beyond a certain point will cause the beam to fail.

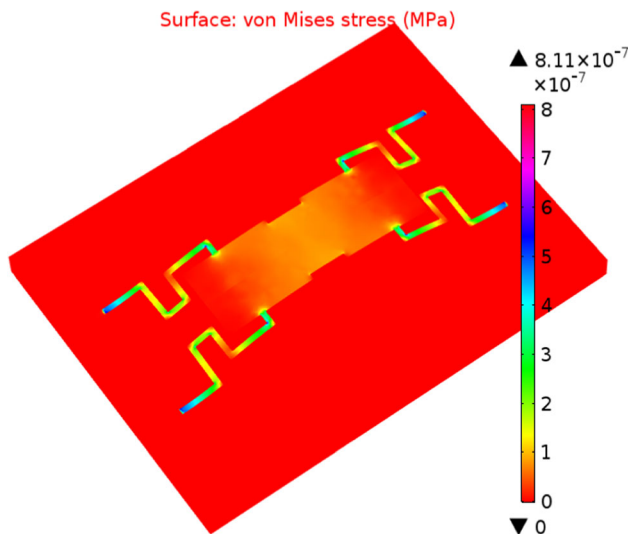


Fig. 10 Stress analysis of the proposed switch

Table 6 Stress analysis with respect to the force

Force units (μN)	Displacement (μm)	Stress (Mpa)
0.5	0.76	2.54
1	1.52	2.27
1.5	2.27	2.27
2	3.03	2.7

The value of critical stress is given by the equation (Chand et al. 2022),

$$\sigma_{cr} = \frac{\pi^2 E t^2}{3l^2(1 - \nu)} \tag{7}$$

where ‘v’ is the poisons ratio of the material and ‘E’ is young modules of the material, ‘t’ is the thickness of beam (Fig. 10).

At initial time when we apply the force on the switch beam material. We got the displacement of 0.76 μm and the stress of 2.54 Mpa as shown in Table 6, when we keep on increasing the force on the switch at a particular point we get more displacement and high stress value.

### 3.2 Electromagnetic analysis

The RF-performance is analyzed in ON and OFF state the switch, in this analysis the S-parameters are measured, which are return loss (S<sub>11</sub>), insertion loss (S<sub>12</sub>), isolation(S<sub>21</sub>).The switch is in ON state the return (S<sub>11</sub>) and insertion loss (S<sub>12</sub>) are generated, in this time the signal will be passes to the input to output. In the OFF state the isolation (S<sub>21</sub>) will be generated.The S-parameters are

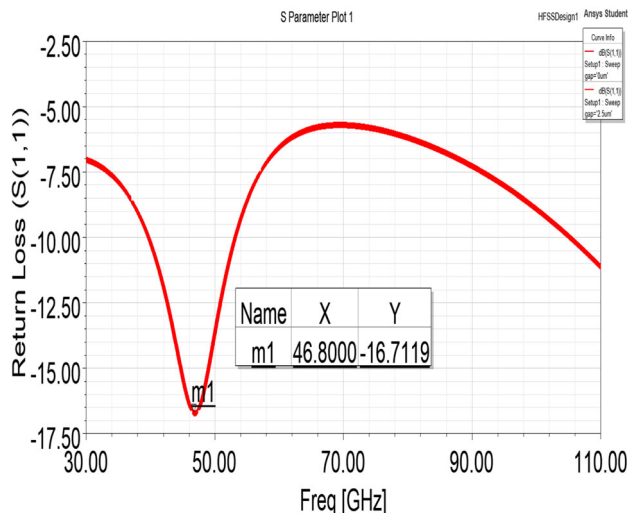


Fig. 11 Return loss of proposed switch

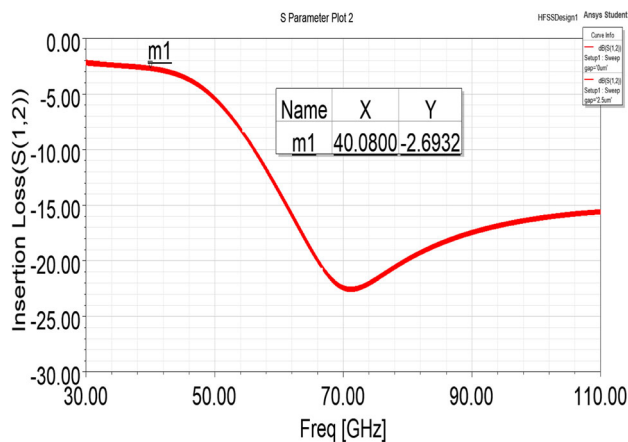


Fig. 12 Insertion loss of proposed switch

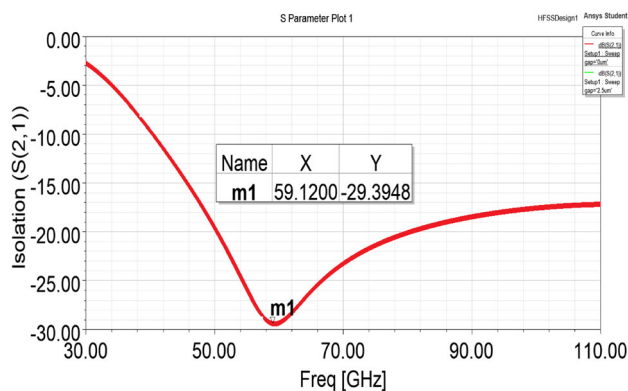


Fig. 13 Isolation measured at 59.12 GHz

calculated in ON and OFF states by using formulas (Sra-vani et al. 2019b; Chand et al. 2021),

**Table 7** S-parameters of the proposed switch

Dielectric thickness (μm)	Return loss (dB)	Insertion loss (dB)	Isolation loss (dB)
0.8	– 16.71	– 2.69	– 29.39
	46.80 GHz	40.08 GHz	59.76 GHz
1	– 18.36	– 5.81	– 19.24
	39.12 GHz	38.82 GHz	39.12 at
1.5	– 16.28	– 33.69 GHz	– 14.58
	34.72 GHz	9.26	33.26 GHz

$$s_{11} = -20\log\left|\frac{-Z_b}{2Z_b + Z_o}\right| \tag{8}$$

$$S_{21} = -20\log\left|\frac{2Z_b}{2Z_b + Z_o}\right| \tag{9}$$

The return, insertion loss, and isolation are simulated in HFSS. The return loss is measured as – 16.71 dB, and insertion loss is – 2.69 dB shown in Figs. 11 and 12. The isolation is obtained as – 29.39 dB at 59.12 GHz frequency as shown in Fig. 13. The S-parameters are obtained at the frequency from 40 to 70 GHz, the S-parameters of the different dielectric thicknesses of S-parameters are analyzed as mentioned in Table 7. Here, we have observed that at 0.8 μm dielectric thickness we have got good RF performance by comparing 1 and 1.5 μm.

### 4 Conclusions

This paper, we have proposed an RF MEMS shunt switch for the v band (40–75 GHz) range used in satellite communication in the VLEO (very lower earth orbit). The RF performance such as return loss, insertion loss, and isolation loss are measured in HFSS tool, the electromechanical analysis such as spring constant, pull-in voltage, capacitance analysis are done by using COMSOL Multiphysics. The switch contributes a low pull-in voltage of 3.3 V. The up and down state of the switch is obtained as 48 fF and 1.19pF. The material’s influence is current on the switch delivering superior execution. The analyzed outputs show that return loss and insertion losses are – 16.71, – 2.69 dB, at 46.80, 40.08 GHz, and isolation of – 29.46 dB at 59.12 GHz. The proposed switch contributes better performance in the V-band range i.e., 40–75 GHz.

**Acknowledgements** The Authors would like to thank to National MEMS Design Centre, NIT Silchar, Assam for providing the necessary tools.

### References

Ansari HR, Khosroabadi S (2019) Design and simulation of a novel RF MEMS shunt capacitive switch with a unique spring for Ka-band application. *Microsyst Technol* 25(2):531–540

Bakri-Kassem M, Mansour RR (2014) High power latching RF MEMS switches. *IEEE Trans Microw Theory Tech* 63(1):222–232

Bansal D, Kumar A, Sharma A, Kumar P, Rangra KJ (2014) Design of novel compact anti-stiction and low insertion loss RF MEMS switch. *Microsyst Technol* 20(2):337–340

Chand CG, Maity R, Maity NP (2021) Electromagnetic modelling and analysis of RF MEMS capacitive shunt switch for 5G applications. *Microelectron J* 117:105262

Chand C, Maity R, Srinivasarao K, Maity NP, Sravani KG (2022) Design and analysis of novel RF-MEMS capacitive type shunt switch for 5G applications. *Trans Electr Electron Mater* 23(1):30–44

Chu C, Liao X, Yan H (2017) Ka-band RF MEMS capacitive switch with low loss, high isolation, long-term reliability and high-power handling based on GaAs MMIC technology. *IET Microwaves Antennas Propag* 11(6):942–948

Demirel K, Yazgan E, Demir Ş, Akın T (2015) A new temperature-tolerant RF MEMS switch structure design and fabrication for Ka-band applications. *J Microelectromech Syst* 25(1):60–68

Dussopt L, Rebeiz GM (2003) Intermodulation distortion and power handling in RF MEMS switches, varactors, and tunable filters. *IEEE Trans Microw Theory Tech* 51(4):1247–1256

Iannacci J (2017) Introduction to MEMS and RF-MEMS: from the early days of microsystems to modern RF-MEMS passives. *Rf-Mems technology for high-performance passives*. IOP Publishing Ltd., Bristol, pp 2053–2563

Lakshmi Narayana T, GirijaSravani K, SrinivasaRao K (2017a) A micro level electrostatically actuated cantilever and metal contact-based series RF MEMS switch for multi-band applications. *Cogent Eng* 4(1):1323367

Lakshmi Narayana T, GirijaSravani K, Srinivasa Rao K (2017b) Design and analysis of CPW based shunt capacitive RF MEMS switch. *Cogent Eng* 4(1):1363356

Lv H, Chen X (2021) New insights into the mechanism of fluid mixing in the micromixer based on alternating current electric heating with film heaters. *Int J Heat Mass Transf* 181:121902

Lv H, Chen X, Zeng X (2021) Optimization of micromixer with Cantor fractal baffle based on simulated annealing algorithm. *Chaos Solitons Fractals* 148:111048

Lv H, Chen X, Wang X, Zeng X, Ma Y (2022) A novel study on a micromixer with Cantor fractal obstacle through grey relational analysis. *Int J Heat Mass Transf* 183:122159

Naji MK, Farhood AD, Ali AH (2019) Novel design and analysis of RF MEMS shunt capacitive switch for radar and satellite communications. *Indones J Electr Eng Comput Sci (IJECS)* 15(2):971–978

- Rao KS, Thalluri LN, Guha K, Sravani KG (2018) Fabrication and characterization of capacitive RF MEMS perforated switch. *IEEE Access* 6:77519–77528
- Rao KS, Naveena P, Sravani KG (2019) Materials impact on the performance analysis and optimization of RF MEMS switch for 5G reconfigurable antenna. *Trans Electr Electron Mater* 20(4):315–327
- Rao KS, Kumar PA, Guha K, Sailaja BVS, Vineetha KV, Baishnab KL, Sravani KG (2021) Design and simulation of fixed–fixed flexure type RF MEMS switch for reconfigurable antenna. *Microsyst Technol* 27(2):455–462
- Sharma K, Karmakar A, Prakash K, Chauhan A, Bansal S, Hooda M, Kumar S, Gupta N, Singh AK (2020) Design and characterization of RF MEMS capacitive shunt switch for X, Ku, K and Ka band applications. *Microelectron Eng* 227:111310
- Singh T, Khaira N, Sengar J (2013) A novel capacitive RF MEMS switch design for low voltage applications. In: 2013 fourth international conference on computing, communications and networking technologies (ICCCNT). *IEEE*, pp 1–6
- Sravani KG, Lakshmi GS, Rao KS (2019a) Design and optimization of piezoresistive materials based microbridge for electro-osmosis pressure sensor. *Trans Electr Electron Mater* 20(3):198–205
- Sravani KG, Prathyusha D, Rao KS, Kumar PA, Lakshmi GS, Chand CG, Naveena P, Thalluri LN, Guha K (2019b) Design and performance analysis of low pull-in voltage of dimple type capacitive RF MEMS shunt switch for Ka-band. *IEEE Access* 7:44471–44488
- Sravani KG, Guha K, Rao KS (2020) A modified proposed capacitance model for step structure capacitive RF MEMS switch by incorporating fringing field effects. *Int J Electron* 107(11):1822–1843
- Vikas K, Sunithamani S, Yagnika M, Siva Krishna S, Avanthi S (2018) Study and analysis of novel RF MEMS switched capacitor. *Int J Eng Technol* 7(1.5):37–41
- Vu TM, Prigent G, Ruan J, Plana R (2012) Design and fabrication of RF-MEMS switch for V-band reconfigurable application. *Prog Electromagn Res B* 39:301–318

**Publisher's Note** Springer Nature remains neutral with regard to jurisdictional claims in published maps and institutional affiliations.